SPATIAL-SPECTRAL CLASSIFICATION OF HYPERSPECTRAL DATA WITH CONTROLLED DATA SEPARATION

Andreia Valentina MICLEA, Mihaela ABRUDAN
Technical University, Faculty of Electronics, Telecommunications and Information Technology, Cluj
andreia.miclea@com.utcluj.ro, abrudan.mi.mihaela@student.utcluj.ro

Abstract: Exploring spatial-spectral data frequently involves classifying hyperspectral images using convolutional neural networks. Due to the high complexity of the data and the scarcity of available training samples, hyperspectral image classification presents significant difficulties. In the context of supervised classification, we find that traditional experimental designs are frequently misused in the spectral-spatial processing context, resulting in unfair or biased performance evaluation, particularly when training and testing samples are selected at random from the same dataset. Under these circumstances, the dependence caused by the overlap between training and testing samples may be artificially increased, in breach of the data independence assumption upheld by supervised learning theory. In order to prevent an unbiased classification result, we present in this paper a controlled strategy designed to minimize the overlap between the samples present in the training and the testing data sets. The proposed controlled sampling strategy ensures a more trustworthy generalization of the CNN model by minimizing the issues present in the random sampling approach, such as the inability to determine whether or not an increase in classification accuracy is due to the spatial information incorporated into a classifier or to an increase in the overlap between training and testing data sets. Experiments performed with a wavelet CNN on different HSIs, namely Indian Pines, Pavia University, and Salinas, ensure the generalization of the data under the assumption that the training and data sets are independent from one another, based on a controlled strategy. Considering the high dimension of the HSI image, as a pre-processing step, the evaluation of the proposed framework is done by PCA and FA methods.

Keywords: *Hyperspectral images, classification, CNN, sampling strategy, hyperspectral image classification, spatial-spectral features, Wavelet.*

I. INTRODUCTION

Machine learning is an important field in image analysis that focuses on self-reliance and independent learning by means of computers and deep learning methodologies to examine various types of data. Unlike machine learning, which uses simpler concepts, in-depth learning employs artificial neural networks, which are designed to mimic how people think and learn in the real world. Even with such state-of-the-art hardware, training a neural network can take a very long time depending on the complexity of the data set and the amount of parameters that make up the network. Deep learning algorithms require a large amount of data in order to deliver trustworthy results [1] .

The field of remote sensing has many uses for hyperspectral imaging (HSI), including studying the atmosphere and monitoring vegetation. The output of hyperspectral sensors includes a wide range of bands with wavelengths from the visible to the near-infrared spectrum, providing rich spectral and spatial information for data analysis. Inadequate spatial data resolution and redundancy are two factors that have a substantial impact on the performance of hyperspectral image classification (HSI), which depends on how data is organized in the spatial and spectral domains [2].

Recent years have seen notable progress in remote sensing thanks to the convolutional neural network (CNN) when data analysis is performed. Regardless of the complexity of their training algorithms and the numerous parameters for the designed network, CNNs have become preferable as effective training and testing methods [3]. Architectures like SVMs, 2D CNNs, 3D CNNs, and 3D-2D CNNs are only a few of the different methodologies that are designed to process large collections of data [4]. Other techniques for manipulating the HSI, aside from 3D-2D CNNs and FuSENet, do not account for the dependencies between the spectral and the spatial data, which typically leads to unsatisfactory performance. Despite the fact that 3D-2D CNNs deal with the spatial and spectral information taken from the HSI cube, their model performance appears to be limited. In comparison to 2D CNNs, 3D CNNs require more computational resources. As a result, the approaches involving only 2D CNN architectures with the ability to extract both spatial and spectral characteristics are preferable.

The SpectralNET [4] architecture, which represents a wavelet CNN, is a variant of the 2D CNN architecture that utilizes spatial and spectral information for multi-resolution HSI classification. This architecture is designed to highlight the spectral features using a wavelet CNN, where the layers are obtained based on the wavelet transform [5]. The decision to use a wavelet transform is based on the fact that it ensures a lesser computation time in comparison with the 3D CNN model. To minimize the high dimension of each data set, the principal component analysis and factor analysis approaches are utilized as a pre-processing phase.

PCA, or principal component analysis, is a scaling approach commonly used to condense large data sets into a manageable amount of variables while maintaining the majority of the data's information [6]. Smaller datasets allow machine learning algorithms to examine data considerably more rapidly and easily since they can be explored and observed more easily [7].

Factor analysis, often known as FA, is a method of

Manuscript received April 3, 2023; revised June 22, 2023

handling data collection and condensing it into a smaller data set that is easier to handle and grasp. It is a method used to determine hidden patterns present in the data, reveal how they interact, and emphasize the traits that many of the patterns in the image share [8]. When dealing with data that has three dimensions or more, PCA or FA are preferable in terms of data reduction methods while preserving the relevant information [6].

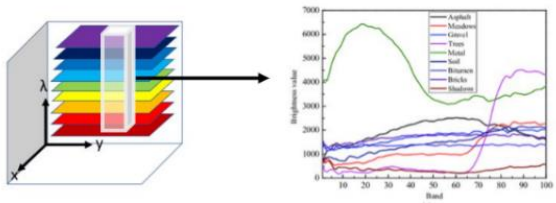

Figure 1. Hyperspectral image representation with spatial and spectral features.

In a supervised learning classification, traditionally, a random sampling selection is used to separate the corresponding samples or add them to the train and to the test data sets for the neural architecture. Different methods were implemented, such as random sampling and various controlled sampling strategies [9], for the high dimensional data sets. In circumstances where we have a relatively small number of samples available in the data sets, the main goal is to achieve the highest classification accuracy possible under those challenging conditions. As previously indicated in [9] and [10], this is an obstacle that deep learning algorithms still need to overcome for spatial-spectral approaches.

This paper is organized as follows. In section II the existing methods for extracting and classifying the data are presented in more detail, along with the sampling strategy. In section III we proposed the classification chain and a controlled strategy for separating the training samples and the testing samples. In section IV the experimental results and the corresponding analysis are described. Section V brings the conclusions.

II. RELATED WORK

A. The spectral–spatial representation of HSI

A hyperspectral image is a three-dimensional data cube, as depicted in Fig. 1, in which the information is distributed along one-dimensional spectral and two-dimensional spatial data. Hyperspectral image sensors have the capability to collect hundreds of spectral channels, resulting in an image composed of N rows, M columns, and B channels. Spectral bands, in particular, express their information over the wavelength ranges, while each individual band incorporates attributes such as shape features and correlation between adjacent pixels in different orientations [11].

We consider the hyperspectral image comprised of many B bands, where each band is stacked on top of the others. In this high dimensional data, each pixel is represented by a collection of attributes, represented by the light intensities dependent on wavelength values.

In the hyperspectral image, every pixel from the data set is represented as a vector with spectral and spatial information. Each value in this vector represents a specific spectral signature selected from the stacked spectral bands.

B. Spectral-spatial architecture for HSI classification

The conventional kernels used in the traditional CNN architecture, known as convolution and pooling layers, are 2D wavelet-derived kernels. As seen in Fig. 2, the SpectralNet framework from [4] is developed on several levels of wavelet decomposition applied on the input HIS patch, with the traditional CNN layers infused with wavelet decomposition. As presented in [12], the wavelet transform has proven that is a good feature extractor for the HSI classification due to its capacity of extracting relevant features from data in a relatively faster manner compared with the traditional convolutional layers.

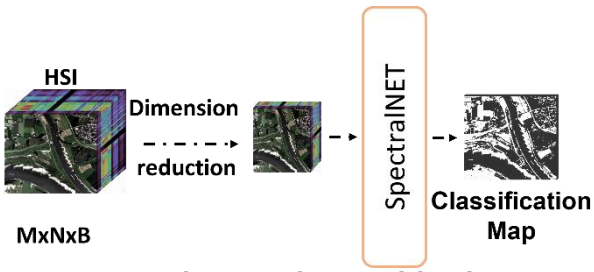

Figure 2. The SpectralNET model architecture.

The spectral and spatial properties from an HSI are therefore revealed when the wavelet transform is combined with the CNN model. These features are then concatenated channel by channel and fed into the 2D CNN's dense classification layers. To lessen the computation burden of classifying the high-dimensionality data, the model uses a pre-processes data stage to reduce the dimension of the data. After the pre-processing step, the selected patches are extracted and fed into CNN. According to [4], the spectral characteristics produced by wavelet transform need less computational effort than a 3D CNN.

Conventional 2D CNNs may be viewed as a constrained form of multi-resolution CNNs that can take into account both spectral and spatial information [13]. A 2D CNN's convolution and pooling layers have been established, based on research [14] as filtering and down sampling. This opens up the possibilities for multi-resolution CNN, in which convolution is done by a pair of wavelet kernels, obtained by extracting the low (L) and high (H) components from the data through a 2D wavelet decomposition.

The Haar wavelet components for the input patch are employed as follows: the low components are used as a scaling function passing from one level to another [15], while the high components are used as kernels for the convolution section [16].

Specifically, the following kernels are utilized:

$$k_{L,L} = \begin{bmatrix} 1 & 1 \\ 1 & 1 \end{bmatrix} \qquad k_{LH} = \begin{bmatrix} -1 & -1 \\ 1 & 1 \end{bmatrix}$$
$$k_{H,L} = \begin{bmatrix} -1 & 1 \\ -1 & 1 \end{bmatrix} \qquad k_{H,H} = \begin{bmatrix} 1 & -1 \\ -1 & 1 \end{bmatrix} \quad (1)$$

In Fig. 3, an example of such a decomposition based on the kernels from equation (1) is illustrated. After the pre-processing is applied, and the dimension of the data is reduced, a patch selection based on a window size is performed. The patches obtained are then sent through the wavelet transform to be decomposed into sub-bands, which are then sent through a convolution layer capable of extracting the features.

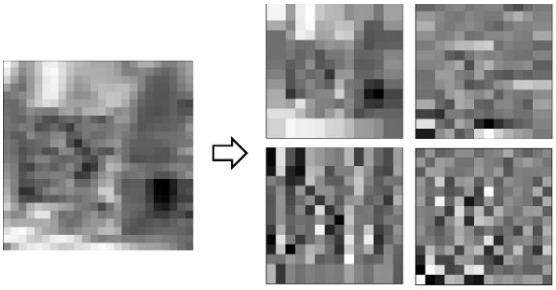

Figure 3. Wavelet decomposition for a patch.

At the subsequent layer, the wavelet transform decomposes the sub-band once more and feeds it to the next stage of the convolution layer. This procedure is carried out for each level, with CNN still gathering spectral and spatial information from the HSI patch. With all the information extracted along the wavelet decomposition and convolution layers; a decision will be made through a dense layer at the end of the model.

C. Controlled Sampling for Classification Accuracy Estimation

Supervised techniques for classifying hyperspectral images focus on clustering hyperspectral pixels or dimensional vectors that belong to the same class based on similar spectral responses or knowing that they may have similar characteristics present in the spatial domain if the pixels are adjacent. On the basis of these assumptions, a trained classifier can be used to predict the labels of previously unseen samples, referred to as the testing data set. However, if the training and testing samples are not carefully chosen, this principle may not always hold true. In the case of supervised classification, the traditional approach for classification results in unfair performance evaluation, which is mainly caused by the random division of the hyperspectral data set into the training and testing samples.

This approach will result in a biased outcome since the testing samples may be spatially adjacent to the training samples. The spatial correlation between the samples indicates that the independence assumption between the train and test data sets is untrue [17]. Due to the presence of highly similar samples in the training data set, this overlapping phenomenon often results in exaggerated classification accuracy, meaning that the information from the testing data set could be employed in the training step. For the spatial operations, we must ensure that the selected patches based on a window size do not overlap with one another, as illustrated in Fig. 4. When employing patch-based representation, as in [18], the independence of the training and testing sets must be taken into account by ensuring a corresponding distance between the patches, from the point of view of the central pixel.

III. PROPOSED ARCHITECTURE

The proposed architecture for HSI classification is the one illustrated in Figure 6, where the CNN 2D wavelet model is used. Therefore, the spatial and spectral information of the hyperspectral images is identified using two methods: the pre-processing stage, namely the Haar wavelet integration, and the 2D CNN model is used.

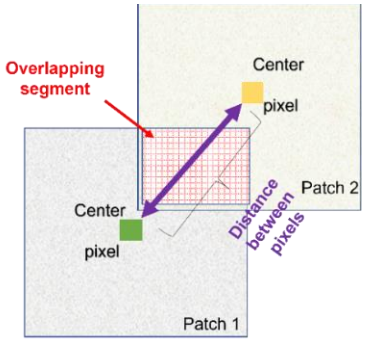

Figure 4. Representation of the overlapping phenomenon: interdependence between the samples in the context of a spatial operation, between two patches centered on a pixel.

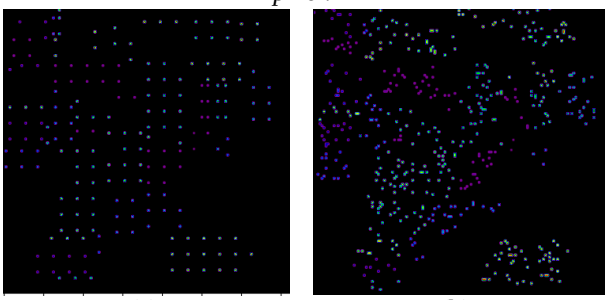

(a) (b)

Figure 5. Example of the training data set samples per class for two selection strategies: (a) controlled sampling, (b) random sampling.

The SpectralNET [4] framework can be separated into 3 stages:

• The first stage is represented by the pre-processing of the data, where a reduction of the dimensionality is implemented. Also in this stage, the data is sectioned in patches based on a given window size.

• In stage two, the selected patch from the previous stage is sent into the wavelet CNN architecture in order to process them through the wavelets, alongside the convolutional layers for the spatial information. At this stage, the patches are chosen at a distance equivalent to the patch dimension, ensuring that in the train data set, we do not have patches that overlap. Each selected patch is then fed to the following stages for 2D wavelet decomposition and convolution layers. This stage of the model has a 4-level wavelet decomposition of the input HSI patch.

•In stage three we have the classification of the obtained vectors from the previous stage with the corresponding labels for the data in question. The patches were selected and labeled as training or testing patches based on the controlled strategy proposed.

The proposed controlled strategy in this paper is based on the dimension of the patches used to extract the information from the data which is then sent into the CNN. For the controlled strategy, we first select a pixel for each class. Starting with the first selected pixel, we add to the training data set, the pixels placed at a distance given by the patch dimensions, in both vertical and horizontal directions. For the newly selected 4 pixels, we will add the next ones considering the same distance previously used. We repeat this process until we reach the number of

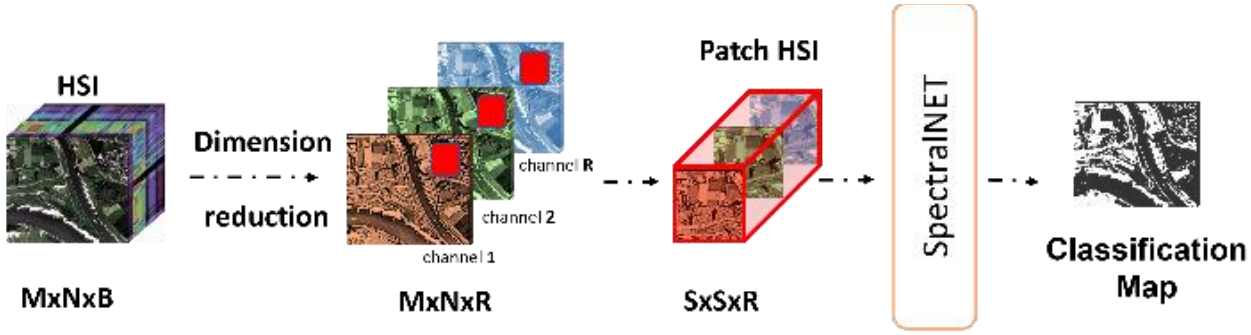

Figure 6. The proposed approach for feature extraction and classification of hyperspectral data.

samples per class or until the point where the number of samples per class, respectively their distribution in the spatial domain forces us to stop the selection of samples, as illustrated in Fig. 5. In this case, from the selected pixel, which is considered the central pixel of the patch, we will construct the 3D patch, in such a manner that the selected patches are placed at a sufficient distance that they will not overlap, ensuring the independence between the training and the data sets. The controlled sampling strategy presented in this paper originates in [18], where the dimension of the window indicates which training samples are selected and placed inside the corresponding window, considering a distance between the windows. The same principle of distance between the training pixels is considered in this research. The selection used in this paper is designed based on the CNN architecture, as illustrated in Fig. 6, which employs 3D windows-sized blocks. Since the training set and the test set must remain independent of one another, the controlled sampling approach described in this study is designed to ensure the independence between 3D blocks selected by the window, based on a central pixel which is considered as a training samples.

IV. EXPERIMENTAL RESULTS

A. Hyperspectral datasets

Three sets of hyperspectral data are used to evaluate the classification's effectiveness: Indian Pines, Pavia University, and Salinas. In the research field of HSI classification, there are available hyperspectral databases [19]. These data sets reflect particularly difficult classification jobs because of the variety of objects present in the data sets, such as small man-made natural structures, and rural and urban regions, which are represented by a smaller number of samples. These databases are commonly used to evaluate the validity and accuracy of different proposed classification approaches [20].

B. Experimental configuration

To prevent the model from overfitting, a global pooling average was added at the end of each convolution layer before sending the data into the dense layer. Our evaluation is based on the SpectralNET model with the corresponding values for the SGD as presented in [14]. In addition, we set the PCA method for the number of components to 10 for all three datasets. For the train and test sample selection, we choose the patches so no overlapping can occur, to ensure the independence between the two data sets for each HSI. The patches evaluated in this section are based on a small size patch, of 3x3 and 5x5 dimensions. The small patch sizes for the controlled strategy generate a slight variation in the number of samples selected for the train and test, compared with the random sampling, since the separation is dimension used in the CNN architecture. conditioned by a distance based on the same patch.

We exploit every class for the three scenes in order to evaluate the efficiency of the proposed classification model. Examining the sample distribution for each data set under the constraint that the neural network needs for the training process large number of samples, we observe an unbalanced distribution of samples per class for Indian Pines. From those 16 classes in total, we have a class with only 20 labels, as the smallest one, and a class with 2455, as the largest one. The Salinas scene features a more diverse and high sample count per class, ranging from 916 to 11271 for the 16 classes. The same distribution is observed in the Pavia University scenario, having a total of 9 classes, where the samples per class range from 947 to 18649. The corresponding distribution of samples in each class will impose a slightly diminished number of samples for the training stage.

C. Results and discussions

The performance indicators employed to evaluate the performance of the proposed classification are Overall Accuracy (OA), Average Accuracy (AA), and Kappa coefficient (Kappa Accuracy) [14]. We evaluate the results for 10 different train and test data sets. For the Indian Pines database, we can evaluate the controlled strategy for sample selection only with the patch size of 3x3 dimension due to the limited number of samples per class. In this case, in Table I, we illustrate only the results for PCA and FA with a random and controlled sampling strategy. The patch size of 3x3 dimension is represented by the scenario in which we can choose only 5% of the samples per class for the random strategy. The small patches are chosen to represent the diversity of each class, regardless of the position of various classes over the spatial dimension.

Analyzing the values from Table I, we can observe that for small samples per class, the two sampling strategies offer similar results in terms of overall accuracy. Also, if we compare the two pre-processing methods, we observe that the FA method performs better than the PCA. We will consider the case of the FA and Wavelet, from Table I, for both random and controlled strategies to analyze further based on the values from Table II, respectively Table III.

If we analyze the detailed classification of the classes for the two sampling strategies, we can observe that we obtain a similar overall classification value of ~ 60%. But if we analyze the precision of each class, we can observe that the controlled sampling, even though with small

samples per class, performs better than the random sampling.

TABLE I. OVERALL ACCURACY (OA%) PCA AND WAVELET VERSUS FA AND WAVELET FOR INDIAN PINES WITH RANDOM, RESPECTIVELY CONTROLLED SAMPLING FOR 3X3 PATCH DIMENSION

	PCA and Wavelet		**FA and Wavelet**	
	OA	**Std.**	**OA**	**Std.**
Random sampling	**59.06**	±0.34	60.77	±0.12
Controlled sampling	58.62	±0.45	**61.5**	±0.68

TABLE II. CLASSIFICATION RESULTS FOR THE INDIAN PINES DATABASE, CONSIDERING A RANDOM SAMPLING TECHNIQUE, WITH FA METHOD AS THE PRE-PROCESSING TECHNIQUE

	precision	recall	f1-score	support
Alfalfa	0	0	0	44
Corn-notill	0.45	0.86	0.59	1357
Corn-mintill	0.77	0.34	0.47	789
Corn	0.31	0.53	0.39	225
Grass-pasture	0.92	0.46	0.61	459
Grass-trees	0.62	0.66	0.64	693
Grass-pasture-mowed	0	0	0	27
Hay-windrowed	0.52	1	0.68	454
Oats	0	0	0	19
Soybean-notill	0.59	0.23	0.34	923
Soybean-mintill	0.71	0.65	0.68	2332
Soybean-clean	0.24	0.23	0.24	563
Wheat	0.97	0.65	0.78	195
Woods	0.92	0.95	0.94	1202
Buildings-Grass-Trees-Drives	0.69	0.29	0.41	367
Stone-Steel-Towers	0	0	0	88
Kappa	55.04772			
Overall	**60.77847**			
Average	42.8903			

This can also be seen in the value of the average accuracy, which goes from ~ 42 % to ~ 53 %. Furthermore, in the case of controlled sampling, we ensure the independence between the training and testing data sets, the classification results obtained without biased data. For Tables IV and V the FA pre-processing method applied before the CNN wavelet gives better results compared with the PCA method. Since we have for Salinas a good distribution for all the classes with a large number of samples per class, we tested the controlled sampling strategy by setting the size of the patch to 5x5. This is also due to the manner in which the data is organized in terms of spatial distribution of classes.

By comparison, for Pavia University we have the same distribution with a larger number of samples per class, but those classes are distributed in the spatial dimension in small areas. Based on the structure of the data, we ensured that we have each class represented over the entire spatial dimension, meaning we established a patch size of 3x3. The good capabilities to ensure a precise classification based on smaller patch sizes with independence between train and test are seen in Table IV for Pavia University, respectively in Table V for Salinas. We examine the results for the hyperspectral data from the perspective of the independence between the training and testing sets, which may account for the benefits of the proposed controlled sampling technique over the random sample one. By analyzing the results from Table IV, respectively Table V, in terms of overall accuracy, the random sampling strategy performs better than the controlled strategy.

TABLE III. CLASSIFICATION RESULTS FOR THE INDIAN PINES DATABASE, CONSIDERING A CONTROLLED SAMPLING TECHNIQUE, WITH FA METHOD AS THE PRE-PROCESSING TECHNIQUE

	precision	recall	f1-score	support
Alfalfa	0.09	0.02	0.04	44
Corn-notill	0.53	0.76	0.62	1395
Corn-mintill	0.72	0.26	0.39	807
Corn	0	0	0	236
Grass-pasture	0.48	0.7	0.57	471
Grass-trees	0.88	0.82	0.85	710
Grass-pasture-mowed	0	0	0	27
Hay-windrowed	0.79	0.93	0.85	471
Oats	0.13	0.61	0.22	18
Soybean-notill	0.5	0.53	0.51	949
Soybean-mintill	0.78	0.59	0.67	2411
Soybean-clean	0.36	0.53	0.43	585
Wheat	0.51	0.48	0.49	202
Woods	0.85	0.73	0.79	1238
Buildings-Grass-Trees-Drives	0.89	0.54	0.67	378
Stone-Steel-Towers	0.17	1	0.29	91
Kappa	56.54307			
Overall	**61.50703**			
Average	53.14251			

TABLE IV. OVERALL ACCURACY (OA%) PCA AND WAVELET VERSUS FA AND WAVELET FOR PAVIA UNIVERSITY WITH RANDOM, RESPECTIVELY CONTROLLED SAMPLING FOR 5X5 PATCH DIMENSION

	PCA and Wavelet		**FA and Wavelet**	
	OA	**Std.**	**OA**	**Std.**
Random sampling	**90.93**	±0.02	**93.39**	±0.41
Controlled sampling	88.5	±0.34	91.92	±0.71

TABEL V. OVERALL ACCURACY (OA%) PCA AND WAVELET VERSUS FA AND WAVELET FOR SALINAS WITH RANDOM, RESPECTIVELY CONTROLLED SAMPLING FOR 3X3 PATCH DIMENSION

	PCA and Wavelet		**FA and Wavelet**	
	OA	**Std.**	**OA**	**Std.**
Random sampling	**88.63**	±0.57	**90.42**	±0.22
Controlled sampling	81.63	±0.48	82.61	±0.95

But those results are misleading, due to the impossibility of ensuring that there is not an overlap between training and testing samples. Overall, the proposed controlled sampling strategy reveals the real discriminative ability of the spectral-spatial wavelet CNN, which is designed to extract small 3D patches containing information in both spatial and spectral dimensions.

The same issue regarding the independence between the training data set and the testing data sets is discussed in [17] and [18]. The mentioned papers discuss the manner in which the spectral-spatial methods usually exploit

information from neighborhood pixels for the same dataset resulting in features that overlap in the spatial domain due to the overlapping of the kernels. The authors from the mentioned papers have offered solutions to ensure the independence between the training and testing data sets, through controlled sampling strategies, as the one presented in this paper. The experimental results from of visual results for FA and Wavelet. As a comparison, for the random sampling technique, in terms of visual results, we have a better representation of the data compared to the controlled sampling technique. But in the case of random sampling, we cannot be sure that we have completely independent samples for the training and data sets.

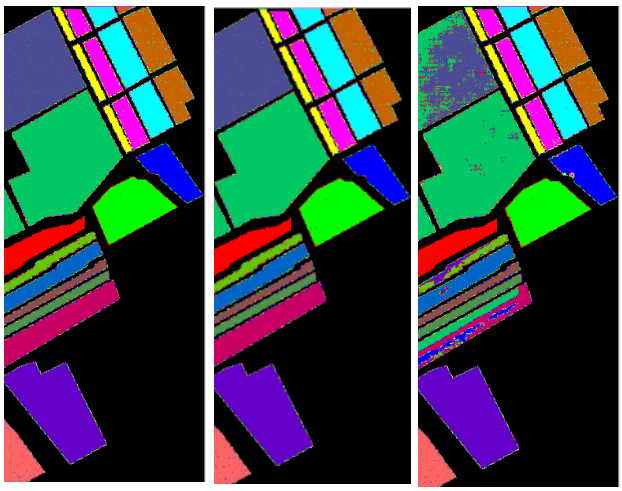

(a) (b) (c)

Figure 7. Comparison of the classification results on the Salinas scene for a patch size of 5x5 and 20% samples per class for training: (a) ground truth of the data set, (b) classification map for sampling strategy, (c) classification map for controlled strategy.

V. CONCLUSIONS

This paper presented the results regarding the impact of the sampling strategy in the context of hyperspectral image classification. Based on the results presented, the issues with random sampling were emphasized, namely that it does not take into account the fact that training and testing samples from the same data set often overlap. Moreover, the implementation of a controlled sampling strategy ensured the independence between the training and testing datasets, enabling reliable evaluation of the model's generalization capabilities. Classifiers developed using convolutional neural network (CNN) architectures that incorporate spectral and spatial information benefit from the controlled sampling technique proposed in this paper.

REFERENCES

[1] Liang. Gao and R. T. Smith, "Optical hyperspectral imaging in microscopy and spectroscopy - a review of data acquisition," *J. Biophoton*, vol. 8, no. 6, pp. 441–456, Jun. 2015.

[2] W. Hu, Y. Huang, L. Wei, F. Zhang, and H. Li, "Deep Convolutional Neural Networks for Hyperspectral Image Classification," *Journal of Sensors*, vol. 2015, pp. 1–12, 2015.

[3] S. Li, W. Song, L. Fang, Y. Chen, P. Ghamisi, and J. A. Benediktsson, "Deep Learning for Hyperspectral Image Classification: An Overview," *IEEE Trans. Geosci. Remote Sensing*, vol. 57, no. 9, pp. 6690–6709, Sep. 2019.

[4] T. Chakraborty and U. Trehan, "SpectralNET: Exploring Spatial-Spectral WaveletCNN for Hyperspectral Image Classification," 2021.

[5] M. Andreia, R. Terebes, and M. Cislariu, "Hyperspectral Image Classification using Extended Local Binary Patterns and Wavelet Transform Descriptors," in *2022 International Symposium on Electronics and Telecommunications (ISETC)*, Timisoara, Romania: IEEE, Nov. 2022, pp. 1–4.

[6] R. Gogineni and A. Chaturvedi, "Hyperspectral Image Classification," in *Processing and Analysis of Hyperspectral Data*, J. Chen, Y. Song, and H. Li, Eds., IntechOpen, 2020.

[7] S. Karamizadeh, S. M. Abdullah, A. A. Manaf, M. Zamani, and A. Hooman, "An Overview of Principal Component Analysis," *JSIP*, vol. 04, no. 03, pp. 173–175, 2013.

[8] J. M. D. Ampong, J. A. Bagares, J. A. Berja, and K. G. Cuarteros, "Factors Affecting Students' E-Learning Activities Using Exploratory Factor Analysis," *CJFY*, vol. 15, no. 1, pp. 90–110, Jan. 2023.

[9] M. E. Paoletti, J. M. Haut, J. Plaza, and A. Plaza, "Deep learning classifiers for hyperspectral imaging: A review," *ISPRS Journal of Photogrammetry and Remote Sensing*, vol. 158, pp. 279–317, Dec. 2019.

[10] S. Jia, S. Jiang, Z. Lin, N. Li, M. Xu, and S. Yu, "A survey: Deep learning for hyperspectral image classification with few labeled samples," *Neurocomputing*, vol. 448, pp. 179–204, Aug. 2021.

[11] L. Tao and A. Mughees, *Deep Learning for Hyperspectral Image Analysis and Classification*, vol. 5. in Engineering Applications of Computational Methods, vol. 5. Singapore: Springer Singapore, 2021.

[12] T. V. N. Prabhakar and P. Geetha, "Two-dimensional empirical wavelet transform based supervised hyperspectral image classification," *ISPRS Journal of Photogrammetry and Remote Sensing*, vol. 133, pp. 37–45, Nov. 2017.

[13] S. Y. Alaba and J. E. Ball, "WCNN3D: Wavelet Convolutional Neural Network-Based 3D Object Detection for Autonomous Driving," *Sensors*, vol. 22, no. 18, p. 7010, Sep. 2022.

[14] S. Fujieda, K. Takayama, and T. Hachisuka, "Wavelet Convolutional Neural Networks," 2018.

[15] Xin Wang, "Moving window-based double haar wavelet transform for image processing," *IEEE Trans. on Image Process.*, vol. 15, no. 9, pp. 2771–2779, Sep. 2006.

[16] P. Liu, H. Zhang, K. Zhang, L. Lin, and W. Zuo, "Multi-level Wavelet-CNN for Image Restoration," in *2018 IEEE/CVF Conference on Computer Vision and Pattern Recognition Workshops (CVPRW)*, Salt Lake City, UT: IEEE, Jun. 2018, pp. 886–88609.

[17] J. Liang, J. Zhou, Y. Qian, L. Wen, X. Bai, and Y. Gao, "On the Sampling Strategy for Evaluation of Spectral-Spatial Methods in Hyperspectral Image Classification," *IEEE Trans. Geosci. Remote Sensing*, vol. 55, no. 2, pp. 862–880, Feb. 2017.

[18] A. V. Miclea, R. M. Terebes, S. Meza, and M. Cislariu, "On Spectral-Spatial Classification of Hyperspectral Images Using Image Denoising and Enhancement Techniques, Wavelet Transforms and Controlled Data Set Partitioning," *Remote Sensing*, vol. 14, no. 6, p. 1475, Mar. 2022.

[19] "Hyperspectral Remote Sensing Scenes - Grupo de Inteligencia Computacional (GIC)." (accessed Jun. 22, 2023).

[20] K. Krishnamurthy, M. Raginsky, and R. Willett, "Multiscale Photon-Limited Spectral Image Reconstruction," *SIAM J. Imaging Sci.*, vol. 3, no. 3, pp. 619–645, Jan. 2010.